치의과학박사 학위논문

Biofilm Removal Effect of MnO_2-Diatom Microbubbler on Inner Surface of Dental Implants

MnO_2-Diatom Microbubbler 의 임플란트 내면 생물막(biofilm) 제거 효과

2023 년 8 월

서울대학교 대학원

치의과학과 치과보철학 전공

김 현 섭

Biofilm Removal Effect of MnO_2-Diatom Microbubbler on Inner Surface of Dental Implants

지도교수 김 명 주

이 논문을 김현섭 박사학위논문으로 제출함

2023 년 6 월

서울대학교 대학원

치의과학과 치과보철학 전공

김 현 섭

김현섭의 박사학위논문을 인준함

2023 년 7 월

위 원 장 _____ (인)

부 위 원 장 _____ (인)

위 원 _____ (인)

위 원 _____ (인)

위 원 _____ (인)

- ABSTRACT -

Biofilm Removal Effect of MnO_2-Diatom Microbubbler on Inner Surface of Dental Implants

Hyunsub Kim, D.D.S., M.S.D.

Department of Prosthodontics, Graduate School, Seoul National University

(Directed by Professor Myung-Joo Kim, D.D.S., M.S., Ph.D.)

***Purpose*:** The increasing popularity of dental implants has led to the emergence of various complications, including peri-implantitis and mechanical issues. While previous studies have focused on the outer surface of implants to treat peri-implantitis, recent research has shown that biofilms on the inner surface of implants is a major contributing factor to peri-implantitis. When MnO_2-Diatom Microbubbler (DM) is treated with hydrogen peroxide, they generate oxygen microbubbles through catalytic reactions and move randomly with propulsion force, resulting in a mechanical removal effect on biofilms. The aim of this study was to evaluate the removal effect of DM on the biofilms formed on the inner surface of dental implant fixtures. Additionally, we evaluated the impact of DM on the mechanical properties of an implant-abutment assembly and investigated its influence on the titanium surface.

***Materials and methods*:** The preparation of DM was performed, and its physicochemical properties were analyzed using a scanning electron microscope (SEM). *Porphyromonas gingivalis* (ATCC 33277), one of the representative anaerobic bacteria causing peri-implantitis, was cultured and inoculated to form a biofilm on the inner surface of the implants. The inner surface of the implants, where the biofilms were formed, was treated with different solutions for 2 minutes, including phosphate-buffered saline (PBS), 0.2% chlorhexidine gluconate (CHX), 3% hydrogen peroxide solution (H_2O_2), and 3% H_2O_2 with 4 mg/mL DM (H_2O_2+DM), followed by rinsing with PBS. To evaluate the viability of the bacteria, a CCK-8 assay was conducted (n = 10), and FITC-conjugated Concanavalin A staining was performed to investigate the extracellular polymeric substances (EPS) of the biofilm (n = 5). The biofilm that remained was examined using scanning electron microscopy (SEM) images and confocal laser scanning microscopy (CLSM). Abutments were connected to the implants in all treatment groups, and reverse torque values were measured (n = 10). X-ray photoelectron spectroscopy (XPS) was used to confirm chemical changes in the titanium disc surface caused by treatment with 3% H_2O_2 and 4 mg/mL DM (n = 4), while CLSM was employed to verify alterations in surface roughness (n = 4). To compare the mean values of each experimental group, one-way analysis of variance (ANOVA) and two-way repeated-measures ANOVA were conducted. Post-hoc analyses using Tukey's test for one-way ANOVA and the Bonferroni method and Tukey's test for two-way repeated-measures ANOVA at a 95% confidence interval were performed.

***Results*:** The co-treatment group of 3% H_2O_2 and 4 mg/mL DM, as well as the 0.2% CHX treatment group, showed a significant decrease in bacterial viability in the biofilms formed on the inner surfaces of the implant compared to other treatment groups. However, the co-treatment group of 3% H_2O_2 and 4 mg/mL DM was found to be more effective in decontaminating the biofilm on the inner surface of the implant, while the 0.2% CHX treatment group showed less effectiveness in removing the biofilms. The co-treatment of H_2O_2 and DM for removing *P. gingivalis* biofilms resulted in a significant increase in reverse torque values in the implant-abutment assembly. Moreover, the co-treatment of H_2O_2 and DM did not affect the physicochemical characteristics of the titanium surface.

***Conclusions*:** The co-treatment of H_2O_2 and DM proved to be a more efficient method for decontaminating *P. gingivalis* biofilms on the inner surface of dental implant fixtures compared to traditional cleaning agents. This highlights the potential for using this novel decontaminator for the inner surface of dental implant fixtures.

Keywords: peri-implantitis, biofilm, manganese oxide, diatom, hydrogen peroxide

Student Number: 2021-37815

CONTENTS

I. INTRODUCTION

Dental implants have been widely recognized as the most successful clinical method for restoring missing teeth over the past four decades.[1] This involves installing an implant fixture into the alveolar bone and connecting implant prosthesis to the fixture after ensuring osteointegration.[2] However, as dental implants have become popular, various complications have also increased. These complications can be categorized as biological complications and mechanical complications.[3] Complications that arise from bacterial infections and affect tissues surrounding the implant fixture are known as peri-implant complications, which include peri-implant mucositis and peri-implantitis.[4] Peri-implantitis is mainly linked to Gram-negative anaerobic bacteria such as *Porphyromonas gingivalis*, *Treponema denticola*, and *Tannerella forsythia*.[5-7] These bacteria create a biofilm around the implant fixture, leading to mucosal inflammation and alveolar bone loss through endotoxin-mediated inflammation.[8] Mechanical complications exist in various forms, including prosthetic screw loosening and prosthetic screw fractures.[3]

Recently, the 2-piece bone-level internal type implant has gained popularity due to its numerous advantages. Compared to the external type implant, which relies only on a screw preload for connection between the implant fixture and the abutment, the internal type implant is connected to an abutment through the friction of a morse taper of the implant fixture and the preload of the screw. This results in less micro-movement, reducing the risk of screw loosening and fracture.[9,10] Additionally, the internal type implant incorporates platform

switching, which causes less marginal bone loss compared to the external type implant that relies on platform matching.[11]

The 2-piece bone-level internal type implant system may have limitations in precision during production, making it difficult to achieve an accurate match between the implant fixture and the abutment.[9] Therefore, fixture-abutment interface (FAI) microgaps may form between the implant fixture and the abutment.[12] Studies have shown that the biofilm from these FAI microgaps can be a significant factor in peri-implantitis.[2,13,14] These microgaps are typically about 4 μm in size, allowing bacteria smaller than this to penetrate and contaminate the internal chamber of the implant fixture, leading to biofilm formation.[15-21] Numerous *in vitro* studies have suggested that bacterial leakage can occur through the FAI microgaps under unloaded conditions.[21-26] Furthermore, these microgaps can expand even more under loading conditions, especially under eccentric loading conditions.[27] Micro-movements of the abutment during use can cause a pumping effect, which drives bacteria through the FAI microgaps.[27] Furthermore, the FAI microgaps may act as a reservoir for anaerobic bacteria such as *P. gingivalis* that cause peri-implantitis.[27,28] Continuous exposure of the peri-implant soft tissue to bacterial exudate from the FAI can cause inflammation, leading to a marginal peri-implant bone loss.[2] This leakage is a significant factor in the development of inflammatory reactions in the area surrounding the implant fixture.[2,13,14] Moreover, biofilms composed of microorganisms, glycoproteins, and extracellular matrices can act as lubricants to decrease the friction.[29] This results in a decrease in the coefficient of friction between the morse taper surface of the bone-level internal

type implant and the abutment, as well as between the prosthetic screw and an inner threaded portion of the implant.[29-31] This reduction in friction adversely affects the mechanical properties of the implant-abutment assembly, such as causing screw loosening and increasing the stress level within the implant-abutment assembly. Therefore, it is crucial to decontaminate the microbial biofilm present on the inner surface of the dental implant fixture.

Various methods have been used to decontaminate bacterial colonization in FAI.[32-35] 0.2% CHX solution has been used for the decontamination of the FAI bacterial colonization.[33] Also, 10% H_2O_2 solution has the potential to remove the internal implant contamination.[36] However, biofilms, which contain an extracellular matrix, limit the access of antibacterial agents, making them more resistant to disinfectants and antibiotics compared to planktonic cells.[37,38] Therefore, it is necessary to study new cleaning methods that can overcome these limitations.

The manganese oxide (MnO_2) nanozyme-doped diatom microbubbler (DM) is a newly developed active cleaning agent. It is created by doping MnO_2 nanozyme sheets on fossilized Aulacoseira diatom particles.[39] When placed in an H_2O_2 solution, the MnO_2 nanozyme sheets on DM generate oxygen microbubbles by decomposing H_2O_2 into water and oxygen through a catalase-imitating activity.[39] These oxygen microbubbles continuously generate an impelling force that causes DM to move randomly and demolish the structure of biofilms.[39] This process is particularly effective in confined spaces, making it a novel therapeutic candidate for decontaminating biofilms on the inner surface of dental implant fixtures.[39]

This study aimed to assess the efficacy of DM in removing biofilms on the inner surface of implant fixtures. Specifically, we compared the ability of DM, CHX, and H_2O_2 to remove *P. gingivalis* biofilms formed on the FAI *in vitro*. The impact of DM on the mechanical properties of an implant-abutment assembly was evaluated.

II. MATERIALS AND METHODS

1. Preparation of DMs

To prepare DM, we followed the method used in a previous study.[39] Specifically, we combined 2 g of diatom particles, 60 mL of toluene, and 0.6 mL of distilled water in a three-necked round-bottom flask equipped with a thermometer, a reflux condenser, and an N_2 gas tube. The mixture was stirred at room temperature for 2 hours, and then we added 3.4 mL of (3-aminopropyl) triethoxysilane (APTES; Sigma-Aldrich, St. Louis, MO, USA). We heated the mixture to 60°C and refluxed it for 6 hours. After cooling down, we washed the mixture with toluene, 2-propanol, and distilled water. We then dried the resulting amine-substituted diatom particles in a vacuum desiccator for 2 days. To further prepare DM, we mixed 0.1 g of the amine-substituted diatom particles with 1 mL of 50 mM potassium permanganate ($KMnO_4$; Sigma-Aldrich, St. Louis, MO, USA). We sonicated the mixture at room temperature for 30 minutes, rinsed the particles with distilled water and ethanol, and then dried them for 24 hours at 60°C in an oven.

2. Physicochemical properties of DMs

To investigate the physicochemical properties of the prepared DMs, we obtained scanning electron microscopy (SEM) images using an Apreo S microscope (Thermo Fisher Scientific, Waltham, MA, USA) at magnifications of 15,000 and 50,000 times at 10.0 kV. We also used an energy dispersive

spectrometer (EDS) in combination with SEM at 20.0 kV to conduct elemental analysis and confirm the successful doping of MnO_2 nanozyme sheets onto the surface of the diatom particles.

3. Biofilm formation on the inner surface of dental implant fixtures

Sterile bone-level internal type implants with a diameter of 4.0 mm and a length of 7.0 mm (Luna; Shinhung, Seoul, Korea) were placed in a 48-well tissue culture plate and inoculated with 1 mL of *P. gingivalis* (ATCC 33277) suspension to form biofilms. *P. gingivalis* was cultured in brain-heart infusion (BHI) broth (Becton, Dickinson and Company, Franklin Lakes, NJ, USA) supplemented with 5.0 mg/mL of hemin (Sigma, St. Louis, MO, USA) and 0.5 mg/mL of vitamin K (Sigma, St. Louis, MO, USA). The bacterial concentration of *P. gingivalis* was adjusted to 2.0×10^8 CFU/mL, based on the standard curve of OD 600 nm versus CFU/mL for *P. gingivalis*. The implants inoculated with *P. gingivalis* were incubated in an anaerobic chamber (10% H_2, 10% CO_2, and balanced N_2) at 37°C for 48 hours.

4. Bacterial viability assay

Fifty sterile bone-level internal type implants were randomly divided into five groups (n = 10). The negative control group received implants in 1 mL of sterile broth, while the other four groups were inoculated with *P. gingivalis* to create biofilms using a previously described method. After 48 hours, the

implants were rinsed with phosphate-buffered saline (PBS, pH = 7.4). The implants with biofilms were then treated with 20 μL of PBS (PBS group), 0.12% (w/v) CHX (Bukwang Pharmaceutical Co., Ltd, Seoul, Korea) (CHX group), 3% (v/v) H_2O_2 (Sigma-Aldrich, St. Louis, MO, USA) (H_2O_2 group), or co-treatment with 4 mg/mL of DM and 3% H_2O_2 (H_2O_2+DM group) for 2 minutes.

The treated implants were then rinsed with PBS before being placed in a 96-well tissue culture plate. The dimensions of this tissue culture plate were suitable for comfortable placement of the implants for subsequent experiments. To assess the viability of the remaining bacteria, 190 μL of sterile BHI broth and 10 μL of bacterial Cell Counting Kit-8 (CCK-8) solution (Dojindo Laboratory, Kumamoto, Japan) were added to another 96-well tissue culture plate. Using a pipette, 20 μL of the BHI broth and CCK-8 solution mixture was added to the internal cavity of the implants. The bacterial suspension was then pipetted and transferred back to the mixture every 30 minutes during a 2-hour incubation period at 37°C. The colored mixture was examined through a bright field imaging using a stereomicroscope (Leica S6D; Leica Microsystems, Wetzlar, Germany) and its absorbance at 450 nm was measured by a microplate reader (Epoch 2; Bio-Tek Instruments, Winooski, VT, USA).

5. Stained biofilm removal assay

A total of 20 bone-level internal type implants were embedded in an acrylic resin block (Ortho-Jet; Lang Dental, Wheeling, IL, USA) and cross-sectioned along their longitudinal axis (Fig. 1(a)) using a cutting machine (Isomet 1000; Buehler, Lake Bluff, IL, USA) (n = 5).[40] The cross-sectioned implants were then reassembled to their original form using flowable composite resin (Denfil Flow; Vericom, Anyang, Korea) and sterilized (Fig. 1(b)). To create biofilms on the inner surface of the implants, a previously described method was used. In order to stain the extracellular polymeric substance (EPS), the implants were placed in BHI broth containing 10 μg/mL of FITC-conjugated Concanavalin A (Sigma, St. Louis, MO, USA) for 20 minutes in a dark cabinet at room temperature. After incubation, the implants underwent a PBS rinse, were re-separated, and then imaged using a fluorescence imaging system (FOBI; Neoscience, Suwon, Korea). The implants were then reassembled with flowable composite resin and placed in a 48-well tissue culture plate, with each group receiving appropriate treatment. Following a PBS wash, the implants were re-separated and imaged again using the fluorescence imaging system. The stained areas in cross-sectional images of the implants ("before treatment" and "after treatment") were measured using image analyzing software (ImageJ; National Institutes of Health, Bethesda, MD, USA).

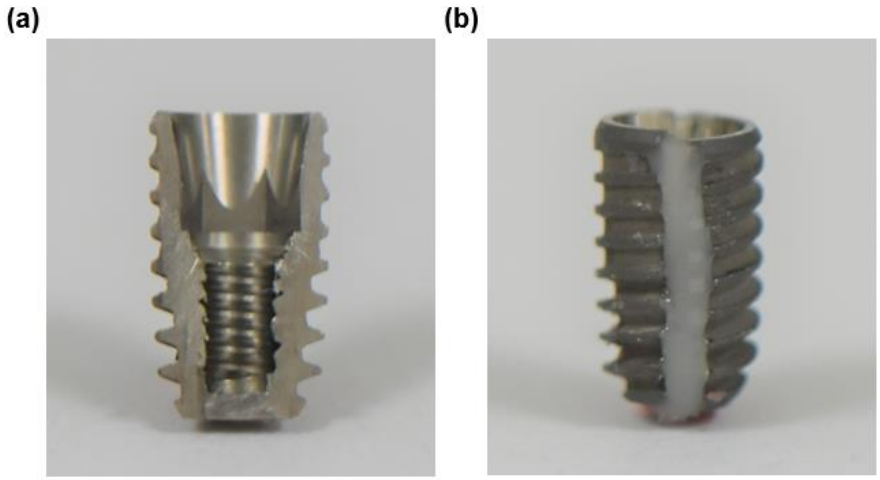

Fig. 1. Cross-sectioned fixture used in the experiment. (a) Images of fixture cross-sectioned along the longitudinal axis. (b) Images of fixture assembled to the original form using flowable composite resin.

6. SEM analysis

The biofilms remaining on the inner surface of cross-sectioned implants were observed using SEM (Apreo S; Thermo Fisher Scientific, Waltham, MA, USA) after each treatment. The specimens were rinsed with PBS and then fixed with 1 mL of 2.5% (v/v) glutaraldehyde for 4 hours. After fixation, the specimens were washed with PBS and dehydrated using a series of ethanol solutions (50%, 70%, 95%, and 100%). Once the specimens had dried completely, they were coated with platinum and visualized using SEM at a voltage of 10 kV to observe the biofilms. The number of bacteria within a 100 μm^2 area in SEM images was measured.

7. CLSM analysis

To assess viability, biofilms on the inner surface of cross-sectioned implants were washed with PBS after each treatment and stained with the Live/Dead BacLight viability kit, which contains SYTO-9 and propidium iodide (Invitrogen, Eugene, OR, USA). The specimens were incubated with the staining solution in a dark cabinet for 20 minutes and then washed with PBS. The cross-sectioned implants were placed with their cut surfaces facing downwards in the bottom of confocal dishes (SPL Life Science, Kyong-Gi, Korea) with BacLight mounting oil (Thermo Fisher Scientific, Waltham, MA, USA). The stained biofilms were imaged using confocal laser scanning microscopy (CLSM) (LSM700; Carl Zeiss, Oberkochen, Germany).

8. Reverse torque test

A total of 50 sterile bone-level internal type implants (diameter: 4.0 mm; length: 7.0 mm; Luna; Shinhung, Seoul, Korea) were randomly assigned to 5 groups, as previously described: negative control group, PBS group, CHX group, H_2O_2 group and H_2O_2+DM group (n = 10). Once the biofilms were formed, the implants were treated according to their respective groups.

The reverse torque value (RTV) was measured using the experimental procedures outlined in a previously published method.[41] Each implant was secured in a customized jig (Fig. 2), and a 4.5 mm diameter, 3.0 mm gingival height Duo abutment (Luna; Shinhung, Seoul, Korea) was connected to the implant. A recommended torque of 30 Ncm was applied to the prosthetic screw with a digital screw torque meter (MGT 50; MARK-10, Copiague, NY, USA). The implant-abutment assemblies were then re-tightened with a torque of 30 Ncm after 10 minutes to account for embedment relaxation. Subsequently, the reverse torque values were measured using the digital screw torque meter.

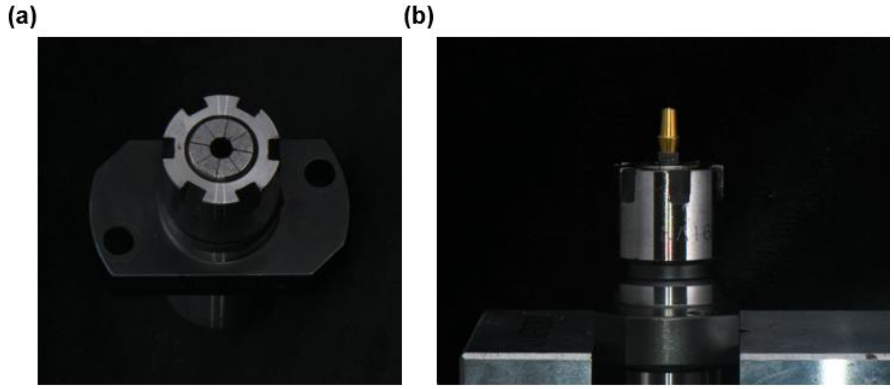

Fig. 2. Customized jig used in the experiment. (a) Images of customized jig. (b) Images of implant-abutment assembly held in a customized jig.

9. Physicochemical characteristics of the titanium disc surface

The machined titanium discs (diameter: 10.0 mm; height: 1.0 mm; Dentium; Seoul, Korea) were treated with double distilled water (DW group), 3% (v/v) H_2O_2 (Sigma-Aldrich, St. Louis, MO, USA) (H_2O_2 group), co-treatment with DW and 4 mg/mL of DM (DW+DM group) or co-treatment with 3% H_2O_2 and 4 mg/mL of DM (H_2O_2+DM group) for 4 minutes (n = 4). After each treatment, titanium discs were cleaned in an ultrasonic cleaner for 5 minutes and then gently wiped and air-dried before analysis. The chemical composition of the titanium disc surfaces was analyzed using X-ray photoelectron spectroscopy (XPS) (Axis Supra; Kratos, Manchester, UK) with monochromatic aluminum X-ray radiation (1486.6 eV). The binding energy scale was calibrated using a reference peak of C 1s (BE = 284.5 eV). The surface roughness of the titanium discs after each treatment was measured using confocal laser scanning microscopy (CLSM) (LSM 800; Carl Zeiss, Jena, Germany). The average surface roughness (Ra) values were calculated over an area of 319 × 319 μm^2.

10. Statistical analysis

The data were determined to follow a normal distribution based on the Shapiro–Wilk normality test ($\alpha = 0.05$), and homogeneity of variance was assessed using Levene's test ($\alpha = 0.05$). A statistical analysis was performed on the quantitative data obtained from the bacterial viability assay, SEM analysis, reverse torque test, and physicochemical characteristics of the titanium disc

surfaces using one-way ANOVA, followed by Tukey's multiple comparison test ($\alpha = 0.05$) as a post-hoc test. The stained biofilm removal assay was analyzed using a two-way repeated-measures ANOVA test ($\alpha = 0.05$). Pairwise comparisons of areas of stained biofilms before and after each treatment were conducted using the Bonferroni method ($\alpha = 0.05$), and comparisons among groups were made using Tukey's multiple comparison test ($\alpha = 0.05$) as a post-hoc test. Statistical analyses were performed using Prism 9 (GraphPad, San Diego, CA, USA).

III. RESULTS

1. Physicochemical properties of DMs

The diatom particles used in this study had a hollow cylinder shape with several pores on their surface (Fig. 3(a) and (b)). An elemental analysis confirmed that MnO_2 nanozyme sheets were evenly incorporated onto the DM surface (Fig. 3(c)).

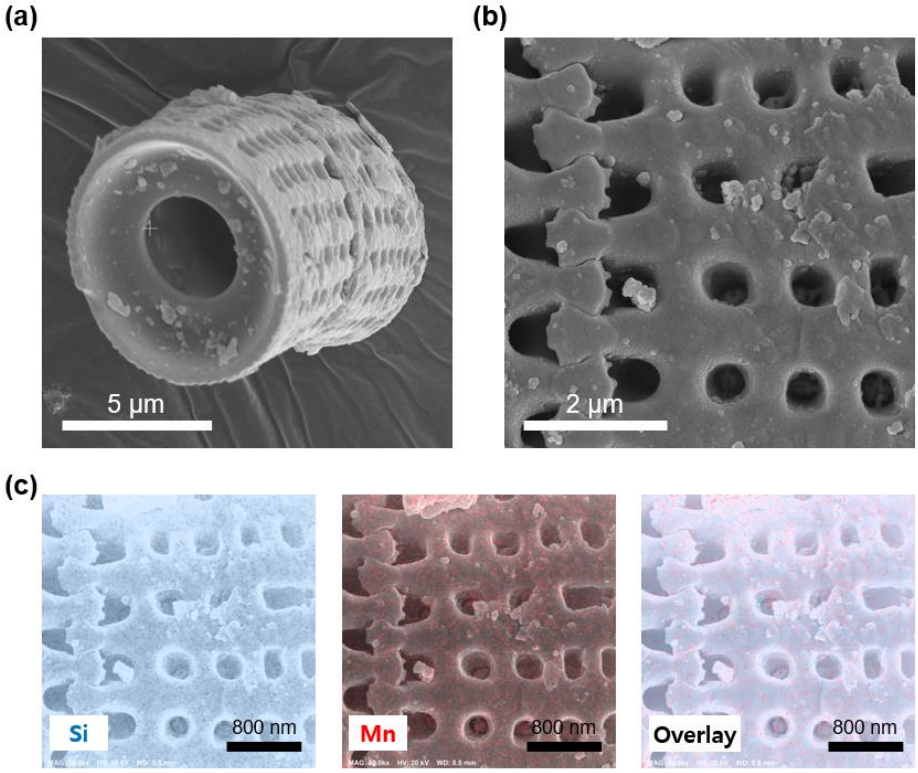

Fig. 3. Scanning electron microscopy (SEM) images and element mapping images of the MnO_2 nanozyme-doped diatom microbubbler (DM) that was fabricated. (a) SEM image of the DM (magnification: 15,000 times, with a white scale bar = 5 μm). (b) SEM image that highlights the pores on the surface of the DM (magnification: 50,000 times, white scale bar = 2 μm). (c) Element mapping images that reveal a uniform distribution of MnO_2 nanozyme sheets on the DM (black scale bar = 800 nm).

2. Bacterial viability assay

The viability of bacteria in biofilms on the inner surface of implants was assessed using CCK-8 after each treatment (Fig. 4). The CHX (0.40 ± 0.03) and H_2O_2+DM (0.36 ± 0.01) groups showed significantly lower levels of an orange-colored product (WST-8 formazan) produced by living bacteria compared to the PBS group (0.68 ± 0.11) ($p < 0.0001$). There was no significant difference between the CHX and H_2O_2+DM groups and the control group (0.38 ± 0.02) ($p > 0.05$), indicating that there were either no viable bacteria or very few in these two groups. The H_2O_2 group (0.70 ± 0.09) did not show a statistically significant difference from the PBS group ($p > 0.05$).

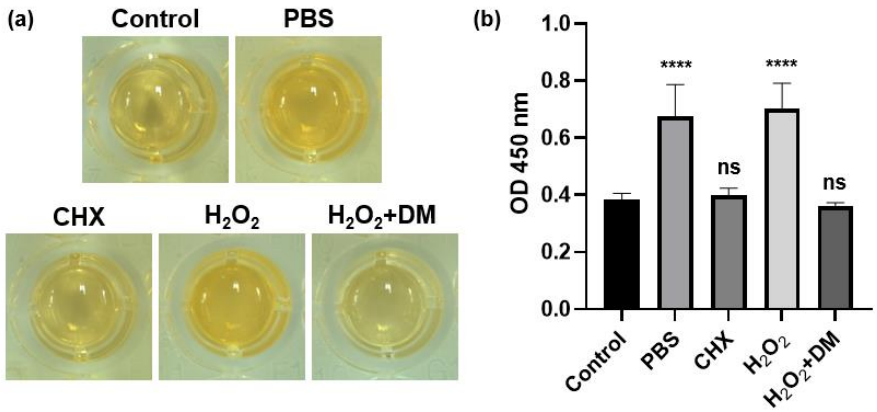

Fig. 4. The viability of *Porphyromonas gingivalis* was assessed using CCK-8. (a) Photographic image of yellow formazan indicating the live bacteria in each group. (b) Quantification of absorbance of samples at 450 nm in Figure 4(a). Data are presented as the mean value ± SD (n = 10). Significance is set to ns, not specific; **: $p \leq 0.01$; ***: $p \leq 0.001$; and ****: $p \leq 0.0001$.

3. Stained biofilm removal assay

The *P. gingivalis* biofilms on the inner surface of the implants were stained with FITC-conjugated Concanavalin A and then photographed and measured before and after each treatment (Fig. 5). Two-way repeated-measures ANOVA was conducted, and Table 1 displays the significance of groups, treatment, and interactions among these factors in the areas of stained biofilms. There was no significant difference in the stained biofilms before and after each treatment in the PBS, CHX and H_2O_2 groups ($p > 0.05$). However, the stained areas of the H_2O_2+DM group significantly decreased after the treatment ($p < 0.0001$).

Table 1. Results of a two-way repeated-measures ANOVA for the area of stained biofilms on the inner surface of the implants before and after each treatment

Source	Sum of square	df	Mean square	F	Sig.
Group (G)	0.7087	3	0.2362	27.84	<0.0001
Treatment (T)	0.2678	1	0.2678	111.00	<0.0001
G x T	0.4661	3	0.1554	64.42	<0.0001
Contaminated area	0.1357	16	0.0085	3.52	0.0081
Residual	0.0386	16	0.0024		

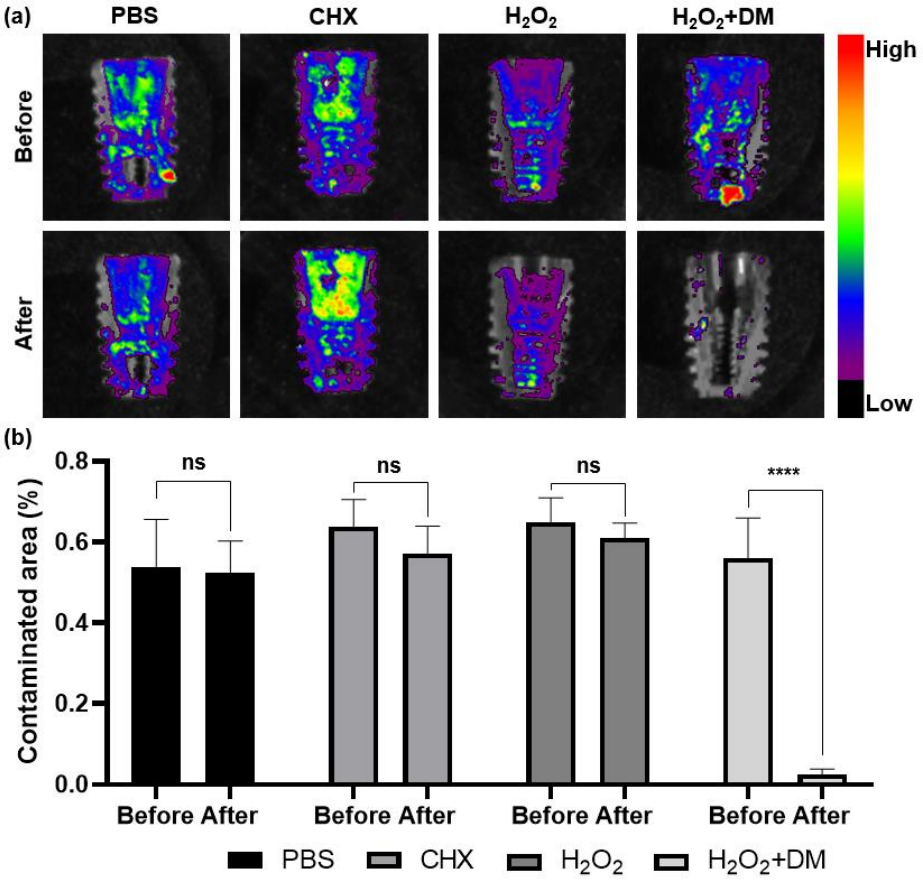

Fig. 5. Decontamination of stained *Porphyromonas gingivalis* biofilms on the inner surface of implants. (a) Relative fluorescence heatmap of FITC-conjugated Concanavalin A stained biofilms before and after each treatment. (b) Stained areas in Figure 5(a) are measured. Data are expressed as mean value ± SD (n = 5). Significance is set to ns, not specific; **: $p \leq 0.01$; ***: $p \leq 0.001$; and ****: $p \leq 0.0001$.

4. SEM analysis

SEM images (Fig. 6(a)) were used to visually investigate *P. gingivalis* biofilms that remained on the inner surface of the implants after each treatment. The CHX and H_2O_2 groups showed similar results to the PBS group, with some bacteria remaining on the inner surface of the implants. However, in the H_2O_2+DM group, only a few bacteria and damaged biofilm residues were observed on the inner surface of the implants. The quantification of the number of bacteria within 100 μm^2 in each group (Fig. 6(b)) reveals no significant difference in the PBS (83.80 ± 21.02), CHX (79.80 ± 33.97) and H_2O_2 groups (80.60 ± 9.94) ($p > 0.05$). However, the H_2O_2+DM group (1.20 ± 1.79) exhibited a very low bacterial count and did not show a statistically significant difference compared to the control group (0.00 ± 0.00) ($p > 0.05$).

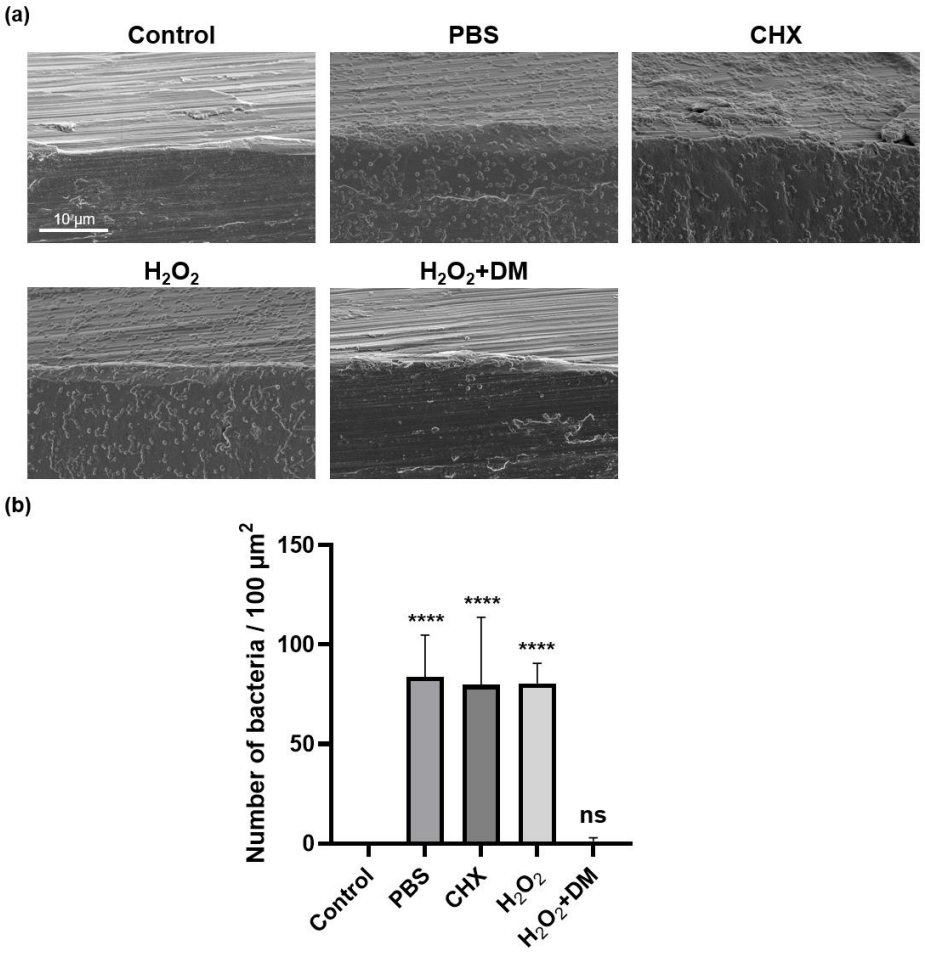

Fig. 6. Scanning electron microscopy (SEM) images of the inner surfaces of the implants after each treatment to remove *Porphyromonas gingivalis* biofilm. (a) The SEM images of each group after decontamination (magnification: 10,000 times, with a white scale bar = 10 μm). (b) Quantification of the number of bacteria within 100 μm^2 in Figure 6(a). Data are presented as the mean value ± SD. Significance is set to ns, not specific; **: $p \leq 0.01$; ***: $p \leq 0.001$; and ****: $p \leq 0.0001$.

5. CLSM analysis

The amount and viability of *P. gingivalis* remaining after treatment were evaluated using CLSM (Fig. 7). The quantity of bacteria remaining in the CHX group was similar to that of the PBS group, but a significant proportion of them were stained red with propidium iodide. The visual representation of the H_2O_2 group was similar to that of the PBS group. However, in the H_2O_2+DM group, only a few bacteria were observed after treatment.

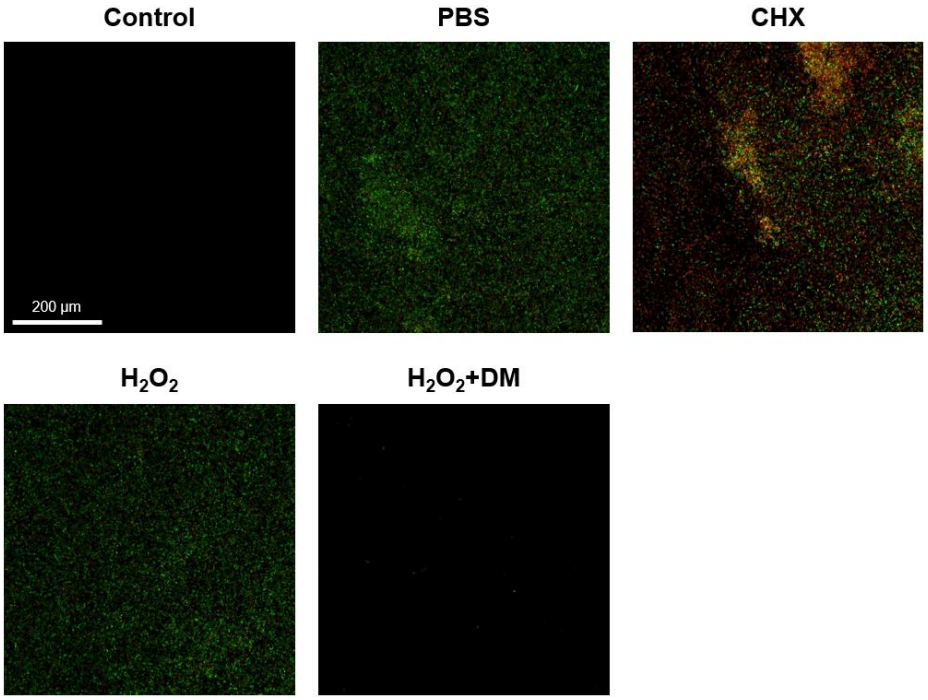

Fig. 7. Confocal laser scanning microscopy images of the *Porphyromonas gingivalis* remaining on the inner surfaces of implants after each treatment. To assess the remaining bacteria and their viability after each biofilm removal treatment, a dual-staining method using SYTO-9/propidium iodide was used. SYTO-9 stains all bacterial cells, while propidium iodide stains dead or damaged bacterial cells.

6. Reverse torque test

After each treatment to remove biofilm from the inner surface of the implants, the abutment was connected to the implant and the reverse torque value was measured (Fig. 8). The mean reverse torque values of the CHX (22.95 ± 0.80 Ncm) and H_2O_2 (22.60 ± 0.91 Ncm) groups were significantly lower than that of the control group (28.10 ± 0.99 Ncm), which was similar to the PBS group (23.35 ± 0.91 Ncm). However, the mean reverse torque value of the H_2O_2+DM group (27.15 ± 1.08 Ncm) was significantly higher than that of the other experimental groups and was similar to the control group.

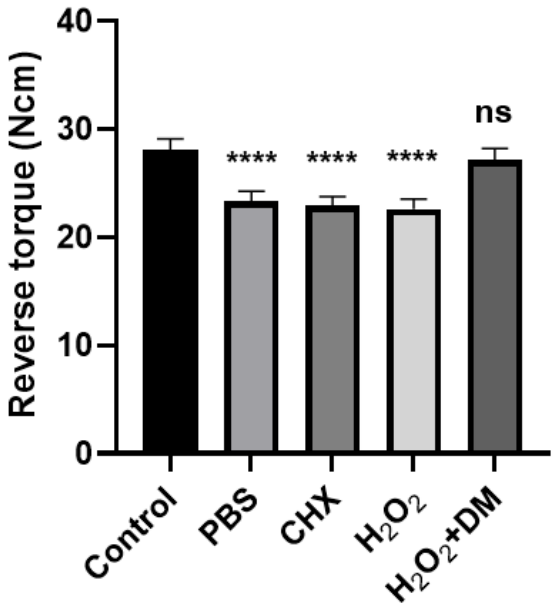

Fig. 8. Reverse torque values for each group. The data are presented as the mean value ± SD (n = 10). The data were analyzed using one-way ANOVA with Tukey's multiple comparison tests ($p < 0.05$). Significance is set to ns, not specific; **: $p \leq 0.01$; ***: $p \leq 0.001$; and ****: $p \leq 0.0001$.

7. Physicochemical characteristics of the titanium disc surface

The study investigated the physicochemical characteristics of machined titanium discs after each treatment (Fig. 9). The average surface roughness (Ra) values were measured using a CLSM (Fig. 9(a)). The Ra values of the H_2O_2 (0.12 ± 0.02 μm), DW+DM (0.12 ± 0.02 μm) and H_2O_2+DM (0.13 ± 0.03 μm) groups were similar to those of the DW group (0.11 ± 0.01 μm) and no significant differences were observed. An XPS analysis was conducted after each treatment to assess any chemical modifications. The XPS results did not show any significant peak shift or change in amplitude (Fig. 9(b)). Additionally, the oxide contents of the H_2O_2 (32.23 ± 1.94 %), DW+DM (34.39 ± 0.80 %) and H_2O_2+DM (35.31 ± 2.05 %) groups were similar to those of the DW group (32.89 ± 0.71 %) and no significant differences were observed (Fig. 9(c)).

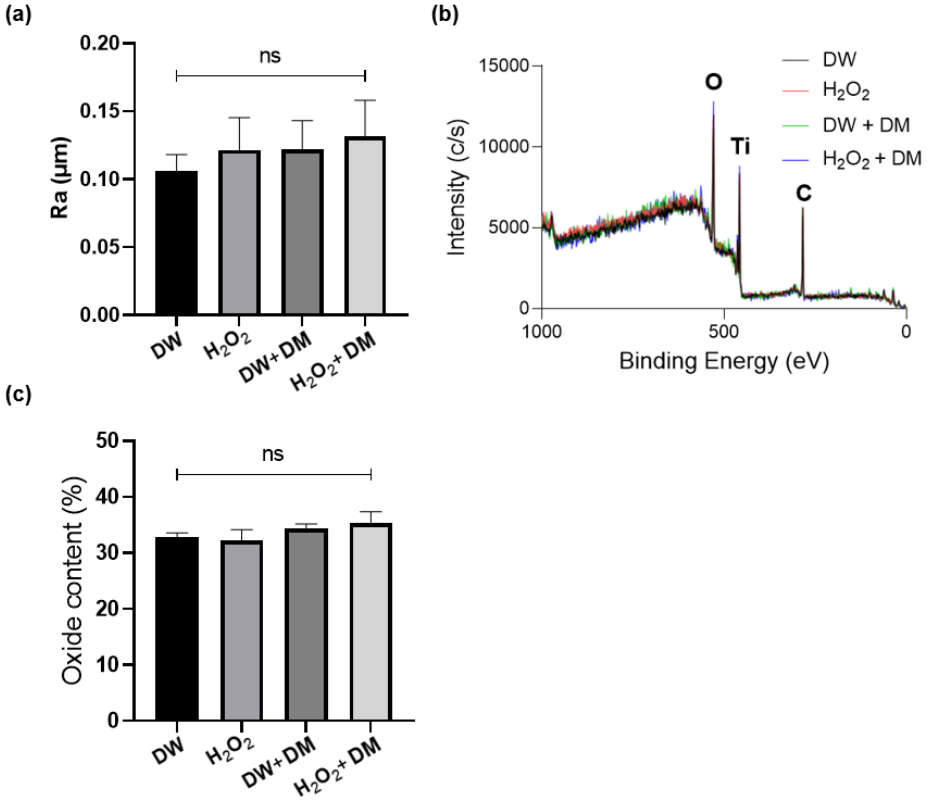

Fig. 9. Physicochemical characteristics of the titanium disc surface after each treatment. (a) Average surface roughness (Ra) values of the titanium discs after each treatment. The data are presented as the mean value ± SD (n = 4). Significance is set to ns, not specific. (b) XPS results of the titanium discs obtained after each treatment. (c) Oxide contents of the titanium discs determined after each treatment. The data are presented as the mean value ± SD (n = 4). Significance is set to ns, not specific.

IV. DISCUSSION

Peri-implantitis is a complex inflammatory condition that poses challenges for both patients and dentists. Research suggests that bacteria can enter the microgaps of the fixture-abutment interface (FAI) and form biofilms, which is a major contributor to peri-implantitis.[2,13,14] One of the primary causative bacteria of peri-implantitis is *P. gingivalis*, which is also found in the FAI microgaps.[27,28] This Gram-negative anaerobic bacterium forms biofilms in the FAI microgaps, leading to inflammation mediated by endotoxins, resulting in mucosal inflammation and marginal bone loss.[8]

Numerous attempts have been made to reduce bacterial colonization on the inner surface of implant fixtures.[32-35] Chlorhexidine (CHX) has been a successful antiseptic for treating periodontal disease for almost 60 years.[42] Previous studies have shown that a 0.2% CHX solution is effective in decontaminating biofilms on the inner surface of implant fixtures.[33] In this study, CHX was found to effectively decrease the viability of *P. gingivalis* (Fig. 4). The viability assay using CCK-8 is an experiment that relies on the fact that living bacteria reduce the colorless WST-8 to form the orange-colored WST-8 formazan.[43,44] When treated with CHX, the orange color of the formazan became lighter, and the absorbance at 450 nm significantly decreased compared to the PBS group, indicating that CHX effectively reduced the viability of *P. gingivalis* in this study. FITC-conjugated Concanavalin A is used to detect glycoproteins in the biofilms of *P. gingivalis* through fluorescent staining. There was no significant difference observed in FITC-conjugated Concanavalin

A staining before and after cleaning with CHX (Fig. 5). In CLSM analysis, SYTO-9 is a green, fluorescent nucleic acid stain commonly used to label live and dead microorganisms, while propidium iodide emits a red fluorescence and can only penetrate cells with damaged membranes, allowing for the visualization of dead and damaged microbes exclusively (Fig. 7).[45,46] Therefore, although CHX can reduce the viability of *P. gingivalis*, it cannot effectively remove dead bacterial cells and the EPS matrix of the biofilms (Fig. 5 and 7).

When H_2O_2 was used alone, there was no significant difference in the viability assay results of *P. gingivalis* biofilms between the H_2O_2 group and the PBS group (Fig. 4). This is because *P. gingivalis* has various defense mechanisms against oxidative stress caused by H_2O_2, such as antioxidant systems[47,48], DNA repair systems[49], and chaperone/protease systems.[50,51] Additionally, *P. gingivalis* has a unique defense mechanism against reactive oxygen species (ROS) damage, which involves obtaining haem on its cell surface.[52,53] This haem, responsible for the black pigmentation of *P. gingivalis*, can lead to the formation of μ-oxo dimers in the presence of ROS, which can catalytically degrade H_2O_2.[53] *P. gingivalis* has genes, including rbr, feoB2, dps, ahpC, and bcp, that provide protection against H_2O_2-induced oxidative stress.[54-59]

The present study assessed the effectiveness of DM as a FAI microgap cleaner, which has the potential to address the limitations of traditional chemical antimicrobial agents. A microparticle called DM has been developed for decontaminating the biofilms. It is created by doping MnO_2 nanozyme sheets onto fossilized Aulacoseira diatom, measuring approximately 10 μm in diameter and 18 μm in length (Fig. 3(a)).[39] It is structured as a hollow cylinder

with walls abundant in pores with an average diameter of 500 nm (Fig. 3(b)).[39] When DM is co-treated with H_2O_2, it produces oxygen through a catalase-like function of MnO_2.[39] The accumulation of oxygen within the cylinder generates pressure, causing DM to move erratically and discharge microbubbles of oxygen.[39] Previous research showed that DM moves at a speed of 60 μm/s when co-treated with a 3% H_2O_2 solution.[39] Utilizing this concept, DM can eradicate the biofilms by infiltrating and moving randomly while continuously generating oxygen gas. Moreover, the oxygen bubbles generated during co-treatment with DM and H_2O_2 can induce oxidative stress in anaerobic bacteria, including *P. gingivalis*.[60] However, *P. gingivalis* may develop resistance to oxidative stress, allowing it to survive in aerobic environments.[61] When forming biofilms, *P. gingivalis* can express the uspA gene and produce the UstA protein to develop a defense mechanism against oxidative stress.[62] After destroying the structure of the biofilm, DM can have a very high bactericidal effect by inducing oxidative stress in a larger contacting area through a large amount of oxygen bubbles. In other words, unlike other chemical agents, DM can have a superior decontamination effect through the synergistic effect of mechanical biofilm destruction and oxidative stress.

DM can overcome the limitations of traditional chemical antimicrobial agents by mechanically disrupting the biofilm structure. While CHX was effective in reducing the viability of *P. gingivalis* (Fig. 4), it failed to effectively remove the EPS of the biofilms (Fig. 5 and 7). Also, H_2O_2 did not significantly decrease the viability of *P. gingivalis* (Fig. 4). SEM analysis revealed that in the CHX and H_2O_2 groups, bacteria were still present on the inner surface of the implant

fixtures, just like in the PBS group (Fig. 6). However, in the H_2O_2+DM group, only a small number of bacteria and residual debris that had been damaged or broken apart were found on the inner surface of the implant fixture (Fig. 6). The presence of lipopolysaccharide (LPS) in the residual EPS can trigger inflammation and hinder proper osteointegration between the implant and the alveolar bone, leading to the development of peri-implantitis.[63-65] The mechanical removal of biofilms using DM can significantly reduce this potential risk.

The biofilms found in the FAI have an impact on the mechanical characteristics of the implant-abutment assembly.[29,30] These biofilms consist of microorganisms, glycoproteins, and EPS, which act as a lubricant, reducing the coefficient of friction between the implant and the abutment and affecting the preload of the prosthetic screw.[29,30] The preload of the prosthetic screw is fundamentally generated by the frictional force between the prosthetic screw and the inner threaded portion of the implant fixture. Therefore, the biofilms formed on the inner surface of the implant fixture also affect the preload of the prosthetic screw.[31] As a result of the decrease in the coefficient of friction, higher stress levels occur in the implant-abutment assembly, which can cause plastic deformation at the implant neck during loading.[31] The present study on reverse torque values shows results consistent with previous experiments (Fig. 8). CHX was effective in killing *P. gingivalis*, but it did not significantly improve reverse torque values compared to the group treated with PBS, as it was unable to remove the biofilm structure (Fig. 8). Similarly, the group treated with H_2O_2 also showed no significant difference in reverse torque values

compared to the PBS treated group, as the lubricating effect of the biofilms was present (Fig. 8). However, DM effectively decontaminated the biofilms, resulting in a significant increase in reverse torque values that were not significantly different from the control group (Fig. 8). Therefore, it can be inferred that when cleaning the FAI with DM, mechanical complications such as screw loosening or fracture will be significantly reduced, and the mechanical properties of the implant-abutment assembly will improve.

Any changes in the mechanical structure or chemical composition of the internal titanium surface of the implant fixture after chemical decontamination could impact the long-term prognosis of the implant-abutment assembly. However, the present study demonstrated that co-treatment with DM and H_2O_2 had no physical or chemical effects on machined titanium discs. Although this experiment was conducted on machined titanium discs for the sake of analysis convenience rather than actual implant fixtures, it is important to note that there is a difference in the pressure generated during the co-treatment of the titanium disc with DM and H_2O_2 compared to the co-treatment of the inner surface of the implant fixture. Considering these limitations, it can be assumed that the inner titanium surface of the implant fixture will also be minimally affected when cleaning the FAI with DM.

In summary, different from conventional chemical agents, DM can remove the biofilms on the inner surface of the implant fixture and destroy the structure of the biofilms, thereby disrupting bacterial resistance and defense mechanisms and this facilitates more effective decontamination. If the DM can only act on the inner space of the implant fixture, the adverse effect on the oral mucosa and

alveolar bone can be minimized, making it a highly promising material for clinical applications. Studies have shown that DM is efficient in removing biofilms in confined areas.[39] To achieve a higher decontamination effect, a stopper can be used to seal the inner space of the implant fixture after co-treating with DM and H_2O_2. Although this *in vitro* study demonstrates the potential of DM as a new therapeutic agent for the decontamination of FAI, further research is needed to determine how DM can be practically used in real-world clinical settings. The characteristics of DM cannot be entirely anticipated through this *in vitro* study since laboratory constraints limit the consideration of all the factors present in an oral cavity. Therefore, caution should be exercised when applying the findings of this study to an in vivo situation. A previous study on mice tongues found that DM did not cause any damage or inflammation to the mucosa and had no adverse effects on MG63 cells.[66] Further research is necessary to investigate the effect of DM on the oral mucosa, including the attached gingiva, in humans.

V. CONCLUSIONS

Our study has shown that co-treatment with H_2O_2 and DM is highly effective in removing *P. gingivalis* biofilms from the inner surface of dental implant fixtures. These results suggest that this approach could be a promising decontamination method for the inner surface of dental implant fixtures. The co-treatment of H_2O_2 and DM was found to be more effective in removing *P. gingivalis* biofilms from the inner surface of dental implant fixtures compared to treatment with CHX or H_2O_2 alone. The study found that the reverse torque values, which had decreased due to the presence of *P. gingivalis* biofilms on the inner surface of dental implant fixtures, were significantly increased after the co-treatment of H_2O_2 and DM. This suggests that decontaminating the inner surface of dental implant fixtures using DM can improve the mechanical characteristics of the implant-abutment assembly. Furthermore, the co-treatment of H_2O_2 and DM did not affect the physicochemical characteristics of the titanium disc surface, including atomic composition, surface roughness, and presence of TiO_2 layers. However, as this *in vitro* study has limitations, further research is necessary to assess the clinical applications of DM for decontaminating the inner surface of dental implant fixtures.

REFERENCES

1. Lang NP. Oral implants: the paradigm shift in restorative dentistry. Journal of Dental Research. 2019;98:1287-93.

2. Sasada Y, Cochran DL. Implant-Abutment Connections: A Review of Biologic Consequences and Peri-implantitis Implications. International Journal of Oral & Maxillofacial Implants. 2017;32:1296-307.

3. Goodacre CJ, Bernal G, Rungcharassaeng K, Kan JY. Clinical complications with implants and implant prostheses. The Journal of Prosthetic Dentistry. 2003;90:121-32.

4. Salvi GE, Cosgarea R, Sculean A. Prevalence and mechanisms of peri-implant diseases. Journal of Dental Research. 2017;96:31-7.

5. Gerits E, Verstraeten N, Michiels J. New approaches to combat Porphyromonas gingivalis biofilms. Journal of Oral Microbiology. 2017;9:1300366.

6. Persson GR, Renvert S. Cluster of bacteria associated with peri-implantitis. Clinical Implant Dentistry and Related Research. 2014;16:783-93.

7. Sharma A. Virulence mechanisms of Tannerella forsythia. Periodontology 2000. 2010;54:106-16.

8. Mombelli A, Müller N, Cionca N. The epidemiology of peri-implantitis. Clinical Oral Implants Research. 2012;23:67-76.

9. Liu Y, Wang J. Influences of microgap and micromotion of implant–abutment interface on marginal bone loss around implant neck. Archives of Oral Biology. 2017;83:153-60.

10. Pjetursson BE, Zarauz C, Strasding M, Sailer I, Zwahlen M, Zembic A. A systematic review of the influence of the implant-abutment connection on the clinical outcomes of ceramic and metal implant abutments supporting fixed implant reconstructions. Clinical Oral Implants Research. 2018;29:160-83.

11. Atieh MA, Ibrahim HM, Atieh AH. Platform switching for marginal bone preservation around dental implants: a systematic review and meta-analysis. Journal of Periodontology. 2010;81:1350-66.

12. Tesmer M, Wallet S, Koutouzis T, Lundgren T. Bacterial colonization of the dental implant fixture–abutment interface: An in vitro study. Journal of Periodontology. 2009;80:1991-7.

13. Harder S, Dimaczek B, Açil Y, Terheyden H, Freitag-Wolf S, Kern M. Molecular leakage at implant-abutment connection—in vitro investigation of tightness of internal conical implant-abutment connections against endotoxin penetration. Clinical Oral Investigations. 2010;14:427-32.

14. Lauritano D, Moreo G, Lucchese A, Viganoni C, Limongelli L, Carinci F. The impact of implant–abutment connection on clinical outcomes and microbial colonization: a narrative review. Materials. 2020;13:1131.

15. Steinebrunner L, Wolfart S, Bößmann K, Kern M. In vitro evaluation of bacterial leakage along the implant-abutment interface of different implant systems. International Journal of Oral & Maxillofacial Implants. 2005;20:875-81.

16. Baj A, Beltramini G, Bolzoni A, Cura F, Palmieri A, Scarano A et al. Bacterial colonization of the implant-abutment interface of conical connection

with an internal octagon: An in vitro study using real-time PCR. Journal of Biological Regulators and Homeostatic Agents. 2017;31:163-8.

17. Cosyn J, Van Aelst L, Collaert B, Persson GR, De Bruyn H. The peri-implant sulcus compared with internal implant and suprastructure components: a microbiological analysis. Clinical Implant Dentistry and Related Research. 2011;13:286-95.

18. Penarrocha-Oltra D, Monreal-Bello A, Penarrocha-Diago M, Alonso-Perez-Barquero J, Botticelli D, Canullo L. Microbial colonization of the peri-implant sulcus and implant connection of implants restored with cemented versus screw-retained superstructures: A cross-sectional study. Journal of Periodontology. 2016;87:1002-11.

19. Romanos GE, Biltucci MT, Kokaras A, Paster BJ. Bacterial composition at the implant-abutment connection under loading in vivo. Clinical Implant Dentistry and Related Research. 2016;18:138-45.

20. Scarano A, Assenza B, Piattelli M, Iezzi G, Leghissa GC, Quaranta A et al. A 16–year study of the microgap between 272 human titanium implants and their abutments. Journal of Oral Implantology. 2005;31:269-75.

21. Jansen VK, Conrads G, Richter E-J. Microbial leakage and marginal fit of the implant-abutment interface. International Journal of Oral & Maxillofacial Implants. 1997;12:527-40.

22. Do Nascimento C, Barbosa R, Issa J, Watanabe E, Ito IY, Junior RA. Bacterial leakage along the implant–abutment interface of premachined or cast components. International Journal of Oral and Maxillofacial Surgery. 2008;37:177-80.

23. Piattelli A, Scarano A, Paolantonio M, Assenza B, Leghissa GC, Di Bonaventura G et al. Fluids and microbial penetration in the internal part of cement-retained versus screw-retained implant-abutment connections. Journal of Periodontology. 2001;72:1146-50.

24. Do Nascimento C, Barbosa RES, Issa JPM, Watanabe E, Ito IY, de Albuquerque Junior RF. Use of checkerboard DNA–DNA hybridization to evaluate the internal contamination of dental implants and comparison of bacterial leakage with cast or pre-machined abutments. Clinical Oral Implants Research. 2009;20:571-7.

25. Barbosa RES, Do Nascimento C, Issa JPM, Watanabe E, Ito IY, de Albuquerque Junior RF. Bacterial culture and DNA Checkerboard for the detection of internal contamination in dental implants. Journal of Prosthodontics: Implant, Esthetic and Reconstructive Dentistry. 2009;18:376-81.

26. Aloise JP, Curcio R, Laporta MZ, Rossi L, Da Silva AMÁ, Rapoport A. Microbial leakage through the implant–abutment interface of Morse taper implants in vitro. Clinical Oral Implants Research. 2010;21:328-35.

27. Cássio do Nascimento D, Paola Kirsten Miani D, Pedrazzi V, Gonçalves RB, Ribeiro RF, Faria ACL. Leakage of saliva through the implant-abutment interface: in vitro evaluation of three different implant connections under unloaded and loaded conditions. International Journal of Oral & Maxillofacial Implants. 2012;27:551-60.

28. Callan DP, Cobb CM, Williams KB. DNA probe identification of bacteria colonizing internal surfaces of the implant-abutment interface: A preliminary study. Journal of Periodontology. 2005;76:115-20.

29. Prado AM, Pereira J, Henriques B, Benfatti C, Magini RS, Lopez-Lopez J et al. Biofilm Affecting the Mechanical Integrity of Implant-Abutment Joints. The International Journal of Prosthodontics. 2016;29:381-3.

30. Sahin C, Ayyildiz S. Correlation between microleakage and screw loosening at implant-abutment connection. The Journal of Advanced Prosthodontics. 2014;6:35-8.

31. Jörn D, Kohorst P, Besdo S, Rücker M, Stiesch M, Borchers L. Influence of lubricant on screw preload and stresses in a finite element model for a dental implant. The Journal of Prosthetic Dentistry. 2014;112:340-8.

32. Duarte AR, Rossetti PH, Rossetti LM, Torres SA, Bonachela WC. In vitro sealing ability of two materials at five different implant-abutment surfaces. Journal of Periodontology. 2006;77:1828-32.

33. Groenendijk E, Dominicus JJ, Moorer WR, Aartman IH, Van waas MA. Microbiological and clinical effects of chlorhexidine enclosed in fixtures of 3I-Titamed® implants. Clinical Oral Implants Research. 2004;15:174-9.

34. Rimondini L, Marin C, Brunella F, Fini M. Internal contamination of a 2-component implant system after occlusal loading and provisionally luted reconstruction with or without a washer device. Journal of Periodontology. 2001;72:1652-7.

35. Besimo CE, Guindy JS, Lewetag D, Meyer J. Prevention of bacterial leakage into and from prefabricated screw-retained crowns on implants in vitro. International Journal of Oral & Maxillofacial Implants. 1999;14:654-60.

36. Jervøe-Storm PM, Hablützel AS, Bartels P, Kraus D, Jepsen S, Enkling N. Comparison of irrigation protocols for the internal decontamination of dental implants—results of in vitro and in vivo studies. Clinical Oral Implants Research. 2021;32:1168-75.

37. Voo ZX, Khan M, Xu Q, Narayanan K, Ng BW, Ahmad RB et al. Antimicrobial coatings against biofilm formation: the unexpected balance between antifouling and bactericidal behavior. Polymer Chemistry. 2016;7:656-68.

38. Flemming H-C, Wingender J. The biofilm matrix. Nature Reviews Microbiology. 2010;8:623-33.

39. Seo Y, Leong J, Park JD, Hong Y-T, Chu S-H, Park C et al. Diatom microbubbler for active biofilm removal in confined spaces. ACS Applied Materials & Interfaces. 2018;10:35685-92.

40. Peñarrieta-Juanito G, Sordi MB, Henriques B, Dotto ME, Teughels W, Silva FS et al. Surface damage of dental implant systems and ions release after exposure to fluoride and hydrogen peroxide. Journal of Periodontal Research. 2019;54:46-52.

41. Cho W-R, Huh Y-H, Park C-J, Cho L-R. Effect of cyclic loading and retightening on reverse torque value in external and internal implants. The Journal of Advanced Prosthodontics. 2015;7:288-93.

42. Löe H, Rindom Schiøtt C. The effect of mouthrinses and topical application of chlorhexidine on the development of dental plaque and gingivitis in man. Journal of Periodontal Research. 1970;5:79-83.

43. Ishiyama M, Miyazono Y, Sasamoto K, Ohkura Y, Ueno K. A highly water-soluble disulfonated tetrazolium salt as a chromogenic indicator for NADH as well as cell viability. Talanta. 1997;44:1299-305.

44. Tominaga H, Ishiyama M, Ohseto F, Sasamoto K, Hamamoto T, Suzuki K et al. A water-soluble tetrazolium salt useful for colorimetric cell viability assay. Analytical Communications. 1999;36:47-50.

45. Chen Y, Wong RW, Seneviratne CJ, Hägg U, McGrath C, Samaranayake LP. Comparison of the antimicrobial activity of Listerine and Corsodyl on orthodontic brackets in vitro. American Journal of Orthodontics and Dentofacial Orthopedics. 2011;140:537-42.

46. Williams S, Hong Y, Danavall D, Howard-Jones M, Gibson D, Frischer M et al. Distinguishing between living and nonliving bacteria: evaluation of the vital stain propidium iodide and its combined use with molecular probes in aquatic samples. Journal of Microbiological Methods. 1998;32:225-36.

47. Pomposiello PJ, Demple B. Global adjustment of microbial physiology during free radical stress. Advances in Microbial Physiology. 2002;46:319-41

48. Lushchak V. Oxidative stress and mechanisms of protection against it in bacteria. Biochemistry (Moscow). 2001;66:476-89.

49. Cadet J, Bourdat A-G, d'Ham C, Duarte V, Gasparutto D, Romieu A et al. Oxidative base damage to DNA: specificity of base excision repair enzymes. Mutation Research/Reviews in Mutation Research. 2000;462:121-8.

50. Shelburne CE, Shelburne PS, Dhople VM, Sweier DG, Giannobile WV, Kinney JS et al. Serum antibodies to Porphyromonas gingivalis chaperone HtpG predict health in periodontitis susceptible patients. PLoS One. 2008;3:e1984.

51. Visick JE, Clarke S. Repair, refold, recycle: how bacteria can deal with spontaneous and environmental damage to proteins. Molecular Microbiology. 1995;16:835-45.

52. Smalley JW, Silver J, Marsh PJ, Birss AJ. The periodontopathogen Porphyromonas gingivalis binds iron protoporphyrin IX in the μ-oxo dimeric form: an oxidative buffer and possible pathogenic mechanism. Biochemical Journal. 1998;331:681-5.

53. Smalley JW, Birss AJ, Silver J. The periodontal pathogen Porphyromonas gingivalis harnesses the chemistry of the μ-oxo bishaem of iron protoporphyrin IX to protect against hydrogen peroxide. FEMS Microbiology Letters. 2000;183:159-64.

54. He J, Miyazaki H, Anaya C, Yu F, Yeudall WA, Lewis JP. Role of Porphyromonas gingivalis FeoB2 in metal uptake and oxidative stress protection. Infection and Immunity. 2006;74:4214-23.

55. Johnson N, McKenzie R, Fletcher H. The bcp gene in the bcp-recA-vimA-vimE-vimF operon is important in oxidative stress resistance in Porphyromonas gingivalis W83. Molecular Oral Microbiology. 2011;26:62-77.

56. Robles A, Reid K, Roy F, Fletcher H. Porphyromonas gingivalis mutY is involved in the repair of oxidative stress-induced DNA mispairing. Molecular Oral Microbiology. 2011;26:175-86.

57. Johnson N, Liu Y, Fletcher H. Alkyl hydroperoxide peroxidase subunit C (ahpC) protects against organic peroxides but does not affect the virulence of Porphyromonas gingivalis W83. Oral Microbiology and Immunology. 2004;19:233-9.

58. Sztukowska M, Bugno M, Potempa J, Travis J, Kurtz Jr DM. Role of rubrerythrin in the oxidative stress response of Porphyromonas gingivalis. Molecular Microbiology. 2002;44:479-88.

59. Ueshima J, Shoji M, Ratnayake DB, Abe K, Yoshida S, Yamamoto K et al. Purification, gene cloning, gene expression, and mutants of Dps from the obligate anaerobe Porphyromonas gingivalis. Infection and Immunity. 2003;71:1170-8.

60. Imlay JA. How oxygen damages microbes: oxygen tolerance and obligate anaerobiosis. Advances in Microbial Physiology. 2002;46:111-53.

61. Henry LG, McKenzie RM, Robles A, Fletcher HM. Oxidative stress resistance in Porphyromonas gingivalis. Future Microbiology. 2012;7:497-512.

62. Kikuchi Y, Ohara N, Sato K, Yoshimura M, Yukitake H, Sakai E et al. Novel stationary-phase-upregulated protein of Porphyromonas gingivalis influences production of superoxide dismutase, thiol peroxidase and thioredoxin. Microbiology. 2005;151:841-53.

63. Jiao Y, Cody GD, Harding AK, Wilmes P, Schrenk M, Wheeler KE et al. Characterization of extracellular polymeric substances from acidophilic microbial biofilms. Applied and Environmental Microbiology. 2010;76:2916-22.

64. Ratcliff PA, Johnson PW. The relationship between oral malodor, gingivitis, and periodontitis. A review. Journal of Periodontology. 1999;70:485-9.

65. Nishio K, Horie M, Akazawa Y, Shichiri M, Iwahashi H, Hagihara Y et al. Attenuation of lipopolysaccharide (LPS)-induced cytotoxicity by tocopherols and tocotrienols. Redox Biology. 2013;1:97-103.

66. Lee EH, Lee SW, Seo Y, Deng YH, Lim YJ, Kwon HB et al. Manganese oxide nanozyme-doped diatom for safe and efficient treatment of peri-implantitis. ACS Applied Materials & Interfaces. 2022;14:27634-50.

– 국문초록 –

MnO_2–Diatom Microbubbler 의 임플란트 내면 생물막(biofilm) 제거 효과

서울대학교 대학원 치의과학과 치과보철학 전공

(지도교수 김 명 주)

김 현 섭

목 적 : 임플란트가 대중화됨에 따라 임플란트 주위염과 기계적 합병증을 포함한 다양한 합병증들이 나타나고 있다. 임플란트 주위염을 치료하기 위해 임플란트 외면 생물막에 대한 많은 연구들이 존재해 왔으나, 최근의 연구는 임플란트 내면의 생물막이 임플란트 주위염의 주요한 기여 인자라고 보고하고 있다. 이산화망간 나노시트가 표면에 입혀진 규조류 미세입자 (MnO_2–Diatom Microbubbler, DM)는 과산화수소수와 함께 처리 시 이를 분해해 아주 작은 크기의 산소 기체 방울을 만들어 내고, 이를 통한 추진력으로 무작위로 움직여 생물막의 물리적인 제거 효과를 나타낸다. 본 연구의 목적은 임플란트 내면에 형성된 생물막에 대한 DM 의 제거 효과를 평가하는 것이다. 뿐만 아니라, DM 의 생물막

제거가 임플란트 지대주 복합체의 기계적 특성에 미치는 영향을 평가하고, DM 이 티타늄 표면에 미치는 영향을 확인한다.

방 법 : 이산화망간 나노시트가 표면에 입혀진 규조류 미세입자 (MnO_2−Diatom Microbubbler, DM)를 제작하고 주사 전자 현미경으로 물리화학적 특성을 분석한다. 임플란트 주위염을 일으키는 대표적인 혐기성 세균 중 하나인 *Porphyromonas gingivalis* (ATCC 33277)를 배양하여 임플란트 내면에 생물막을 형성한다. 생물막이 형성된 임플란트 내면은 인산완충 생리식염수 (PBS), 0.2% 클로르헥시딘 글루코네이트 (CHX), 3% 과산화수소수 (H_2O_2), 그리고 3% H_2O_2 와 4 mg/mL DM (H_2O_2+DM)으로 각각 2 분씩 처리 후 PBS 로 세척되었다. 각 처리 군의 남아 있는 세균의 생존력 측정을 위해 CCK−8 염색 실험을 시행하였고 (n = 10), 생물막의 세포 외 고분자물질을 확인하기 위해 FITC−conjugated Concanavalin A 염색을 시행하였다 (n = 5). 주사 전자 현미경 영상, 공초점 레이저 주사 현미경 영상을 통해 각 처리 군의 남아있는 생물막을 분석하였다. 각 처리 군의 임플란트에 지대주를 연결하고 나사 풀림 토크 값을 측정하였다 (n = 10). 3% H_2O_2 와 4 mg/mL DM 처리로 인한 티타늄 디스크 표면에 미치는 화학적 영향을 알아보기 위해 X 선 광전자 분광법을 (n = 4), 표면 거칠기를 측정하기 위해 공초점 레이저 주사 현미경을 사용하였다

(n = 4). 각 실험 군의 평균값 비교를 위해 일원배치 분산분석과 이원배치 반복측정 분산분석을 시행하였고, 일원배치 분산분석은 Tukey's test 를, 이원배치 반복측정 분산분석은 Bonferroni method 와 Tukey's test 사용하여 신뢰구간 95%에서 사후분석 하였다.

결 과 : 3% H_2O_2 와 4 mg/mL DM 을 함께 처리한 군과 0.2% CHX 로 처리한 군이 다른 처리 군들과 비교했을 때 임플란트 내면 세균이 가장 적게 살아남아 있었다. 하지만, 3% H_2O_2 와 4 mg/mL DM 을 함께 처리한 군은 임플란트 내면 생물막 자체를 효과적으로 제거한 반면, 0.2% CHX 처리 군은 생물막의 제거에는 효과를 보이지 않았다. 3% H_2O_2 와 4 mg/mL DM 을 함께 처리한 군은 다른 군들에 비해 유의미한 나사 풀림 토크 값의 증가를 나타냈다. 3% H_2O_2 와 4 mg/mL DM 을 함께 처리함으로 인한 티타늄 표면의 물리화학적 변화는 확인되지 않았다.

결 론 : *P. gingivalis* 세균을 사용한 실험에서, 과산화수소수와 DM 을 함께 처리하는 치료법은 전통적인 화학 세정제들로 처리하는 것에 비해 임플란트 내면의 생물막을 효과적으로 제거하였다.

주요어 : 임플란트 주위염, 생물막, 이산화망간, 규조류, 과산화수소
학 번 : 2021-37815